WEP Warwick Evans Publishing

International Journal of Natural Resources and Environmental Studies

ISSN: 3006-2012 (Print), ISSN: 3006-0834 (Online) | Volume 6, Number 1, Year 2025
DOI: https://doi.org/10.62051/ijnres.v6n1.03
Journal homepage: https://wepub.org/index.php/IJNRES/index

Modeling of Tunnel Advanced Geological Prediction and Forward Simulation of Seismic Wave Propagation

Shengyuan Jia

School of Resources and Environment, Henan Polytechnic University, Jiaozuo 454000, China

ABSTRACT

With the rapid development of transportation infrastructure in China, an increasing number of railway, highway, and urban rail transit projects have emerged like bamboo shoots after rain. Nevertheless, many tunnel projects still face significant challenges during construction, which constrain overall transportation development. In tunnel engineering, adverse geological formations such as fractured zones, karst caves, and faults are frequently encountered. Failure to detect these hazardous geological bodies in a timely manner and implement appropriate construction measures may not only delay project progress but also pose serious threats to the safety of construction personnel. Tunnel advanced geological prediction technology, employing the seismic reflection method, provides accurate characterization of geological conditions near the tunnel face. As an approach for advanced detection, wavefield forward simulation offers convenience and precision. However, reliable forward simulation requires accurate geological models. Therefore, this study focuses on analyzing the characteristics of various geological models and develops a programmatic approach to generate these models to meet the requirements of forward simulation. Finally, the wavefield characteristics are comparatively analyzed based on the forward simulation results derived from the geological models.

KEYWORDS

Geological Modeling Wavefield Forward Modeling.

1. INTRODUCTION

In recent years, with the rapid development of China's national economy and the large-scale construction of high-speed railways, expressways, and urban rail transit projects, the number of long tunnels has increased significantly[1].

During tunnel construction, frequently encountered unmapped geological formations not only progressively increase project costs but may also lead to catastrophic accidents, endangering workers' lives and causing significant economic lossesv[2]; therefore, effective detection of minor geological structures before excavation is crucial.Advanced geological prediction enables timely identification of anomalies, accurately forecasting the location, occurrence, and structural integrity of adverse geological bodies ahead of the tunnel face, as well as potential water-bearing conditions[3]; this provides critical basis for proper selection of excavation cross-sections[4]; determination of support parameters; and optimization of construction schemes[5].The technology also delivers early warnings for potential disasters like water inrush, mud outbursts, and gas explosions, allowing contractors to take preventive measures and ensure construction safety while achieving significant cost savings[6].Tunnel advance prediction thus offers substantial social and economic benefits, including safer construction practices[7]; enhanced work efficiency; shortened project duration; accident prevention; and reduced investment costs[8].

Various geological models are established by configuring three fundamental parameters - P-wave velocity, S-wave velocity and density - across different rock strata to construct physical models for forward simulation[9]; the forward modeling program subsequently generates synthetic seismic datasets under these predefined parameter configurations; these simulated data undergo preliminary processing to produce seismic time-profile curves for detailed wavefield characteristic analysis[10].

The research employs a comparative methodology beginning with comprehensive analysis of a 3D baseline model without geological anomalies[11]; this initial phase systematically examines seismic record images and characteristic snapshots of key profiles to establish fundamental understanding of channel wave components in the construction zone[12]; this baseline investigation provides the necessary reference framework for subsequent study of channel wave behavior in models containing unidentified geological structures.Wavefield analysis follows a structured approach where the baseline model examination treats each component's seismic records and corresponding snapshots as independent study units; in contrast, the anomalous model investigation adopts a paired comparative approach, grouping corresponding channel wave components from both models for direct comparison; this methodological design specifically isolates and highlights the perturbing effects of geological anomalies on channel wave propagation through systematic differential analysis[13].

2. ESTABLISHMENT OF 3D MODELS FOR SEISMIC WAVE ADVANCED DETECTION

MATLAB is adopted for implementing the 3D scalar data volume due to its superior matrix operation capabilities; to construct effective forward modeling-ready models, the data storage must follow specific organizational principles; the implemented storage sequence prioritizes x-axis data, followed by y-axis, and finally z-axis coordinates.The core methodology constructs the 3D scalar data volume by utilizing matrix elements to represent both formation density and seismic wave propagation velocities; the inherent row-column-page structure of 3D matrices inherently defines spatial relationships between data points; model configuration is achieved by modifying specific matrix element values at targeted spatial locations, thereby resolving both data assignment and structural arrangement challenges.The following code segment demonstrates the implementation of a karst cave model:

```
xmax_base=str2double(get(handles.x,'string'));
ymax_base=str2double(get(handles.y,'string'));
zmax_base=str2double(get(handles.z,'string'));
vp_base=str2double(get(handles.vp_base,'string'));
vs_base=str2double(get(handles.vs_base,'string'));
rho_base=str2double(get(handles.rho_base,'string'));
vp_rd=str2double(get(handles.p_vp,'string'));
vs_rd=str2double(get(handles.p_vs,'string'));
rho_rd=str2double(get(handles.p_rho,'string'));
r_xx=str2double(get(handles.r_x,'string'));
r_yy=str2double(get(handles.r_y,'string'));
r_zz=str2double(get(handles.r_z,'string'));
r_r=str2double(get(handles.r_r,'string'));
sl=str2double(get(handles.s_l,'string'));
```

```
sr=str2double(get(handles.s_r,'string'));
a=ymax_base/2-sr;
b=ymax_base/2+sr;
c=zmax_base/2-sr;
d=zmax_base/2+sr;
e=r_xx-r_r;
f=r_xx+r_r;
g=r_zz-r_r;
h=r_zz+r_r;
i=r_yy-r_r;
j=r_yy+r_r;
vp_tunnel=0.0;
vs_tunnel=0.00001;
rho_tunnel=1.25;
mod=(zeros(xmax_base,ymax_base,zmax_base));
mod(:,:,:)=vp_base;
mod(e:f,g:h,i:j)=vp_rd;
mod(1:sl,a:b,c:d)=vp_tunnel;
mod=permute(mod,[2 1 3]);
fid_mod=fopen(strcat('model_rongdong','.vp'),'w');
fwrite(fid_mod,mod,'float');
fclose(fid_mod);
mod1=(zeros(xmax_base,ymax_base,zmax_base));
mod1(:,:,:)=vs_base;
mod1(e:f,g:h,i:j)=vs_rd;
mod1(1:sl,a:b,c:d)=vs_tunnel;
mod1=permute(mod1,[2 1 3]);
fid_mod1=fopen(strcat('model_rongdong','.vs'),'w');
fwrite(fid_mod1,mod1,'float');
fclose(fid_mod1);
mod2=(zeros(xmax_base,ymax_base,zmax_base));
mod2(:,:,:)=rho_base;
mod2(e:f,g:h,i:j)=rho_rd;
mod2(1:sl,a:b,c:d)=rho_tunnel;
mod2=permute(mod2,[2 1 3]);
fid_mod2=fopen(strcat('model_rongdong','.rho'),'w');
```

```
fwrite(fid_mod2,mod2,'float');
fclose(fid_mod2);
```

The presented code exhibits distinct implementation characteristics compared to standard m-files; within MATLAB's GUI environment, interactive systems are constructed through incorporation of multiple controls possessing various properties; among these, the 'Tag' property functions as a unique identifier analogous to personal identification, serving as a critical internal recognition attribute.All control properties are systematically consolidated within the handles data structure; this structure operates as a centralized repository for property management; user-input data access requires targeted retrieval of string data from this repository using specific Tag identifiers; this methodology facilitates complete data transfer into the program's processing core.A critical development consideration remains imperative; user-acquired data through this method maintains character-type (string) formatting; when employed for matrix element assignment, explicit conversion to numerical-type variables becomes mandatory; neglecting this conversion will generate program execution faults; proper implementation requires str2double() or str2num() functions with complementary validation checks.

The next step involves assigning values to the elements of the 3D matrix; the core approach for creating the 3D scalar data volume uses matrix elements to simulate both formation density and seismic wave propagation velocities; however, a conflict arises because forward modeling requires row-major storage while MATLAB defaults to column-major storage.To resolve this discrepancy, the permute function must be applied to rearrange the matrix dimensions after element assignment; this requirement leads to unconventional matrix indexing during initialization; traditionally, mod(:,:,:) represents rows, columns, and pages, but for this model, it must instead be interpreted as rows, pages, and columns.Only by assigning values under this revised indexing scheme can the permuted matrix properly meet forward simulation requirements; this adaptation ensures correct data alignment while maintaining geological accuracy.

The karst cave modeling process initiates with creating a 3D matrix matching the model dimensions; all matrix elements are initially assigned the P-wave velocity parameters of surrounding rock; user-input data then calculates the cave's dimensions and corresponding matrix indices; these indices locate target elements for reassignment with fracture zone P-wave velocities.The tunnel structure is incorporated into this model using identical methodology; final processing involves dimensional reorganization per previously specified requirements; the restructured matrix undergoes binary file conversion for disk storage; this preservation protocol ensures data integrity for subsequent simulations.Parallel procedures generate corresponding 3D scalar volumes for S-wave velocities and density distributions; parameter variation enables vertical stratum modeling through systematic value reassignment; each geological feature maintains independent parameterization while sharing the core computational framework.

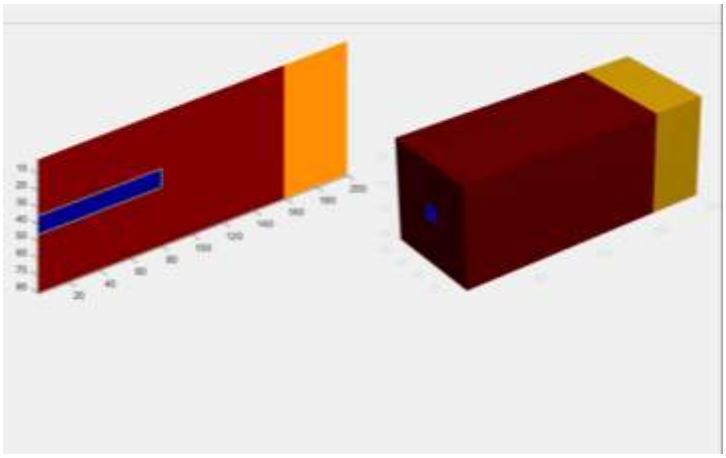

FIG 1. vertical stratigraphic model

Similarly, fracture zone models can be obtained by configuring different parameters; this involves adjusting P-wave/S-wave velocities and density values to characterize rock fracturing; the modeling process maintains the same technical workflow as the karst cave implementation; all matrix operations and storage protocols remain consistent while accommodating geological variations.

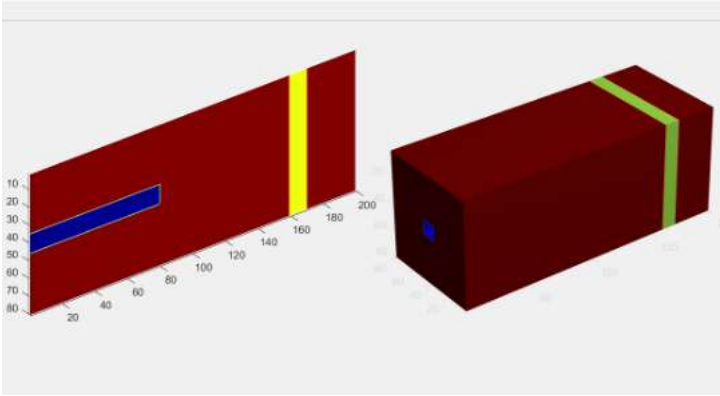

FIG 2. crushing zone model

The partial code for implementing the fault model is as follows:

```
mod=(zeros(xmax_base,ymax_base,zmax_base));
mod(:,:,:)=vp_base;
for i=1:zmax_base
    mod(1:ys,i,:)=vp_rd;
    ys=ys+1;
end
mod(1:sl,a:b,c:d)=vp_tunnel;
mod=permute(mod,[2 1 3]);
fid_mod=fopen(strcat('model_duanceng','.vp'),'w');
fwrite(fid_mod,mod,'float');
fclose(fid_mod);
```

In this code, there are changes in the assignment of the fault. During the model creation process, the starting position of different geological bodies is controlled by the parameter ys. The fault is simulated by incrementing ys. Specifically, the assignment is done page by page. For example, on the first page, the elements to be assigned are located from the first row to the ys-th row and from the first column to the last column; on the second page, the elements to be assigned are located from the first row to the ys + 1-th row and from the first column to the last column, and so on. This continues until i reaches the maximum value, and the assignment of the fault is completed. Finally, the matrix is written into a binary file in the original storage format and saved on the computer.

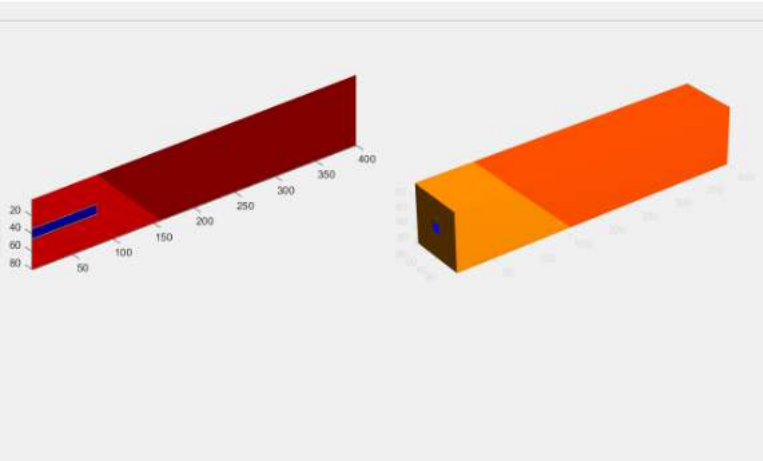

FIG 3. fault model

The implementation of the display model function in the three - dimensional geological modeling system is different from the process of creating a model. In terms of display, MATLAB provides functions such as plot3, slice, and patch. For data reading, one first needs to know the size of the data volume and the name of the data volume, which can be input by the user and then passed into the program. At this moment, the data volume is read and its data is stored in a new matrix, which is exactly the opposite process of model building. The partial code for reading the data volume is as follows;

```
function Vol = GetBin3DData(FileName,InLineLen,CrossLineLen,SampleLineLen)
Vol = zeros(InLineLen,CrossLineLen,SampleLineLen);
fid = fopen(FileName);
for i = 1:1:InLineLen
    for j = 1:1:CrossLineLen
      if(i == InLineLen && j == CrossLineLen)
       return;
      end
      [Vol(i,j,:), nCount] = fread(fid,SampleLineLen,'float');
      if(nCount ~= SampleLineLen)
        fprintf('error！ ');
      end
    end
end
fclose(fid);
end
```

The main function of this function is to read the three-dimensional scalar binary data volume into the Vol matrix. Then comes the display part. Part of the code is as follows:

```
[x,y,z]=meshgrid(1:CroLine,1:InLine,1:TimeLine);
axes(handles.axes1);
slice(x,y,z,Vol,[],ymax_base/2,[]);
```

```
shading interp
set(gca,'zdir','reverse');
axis equal
grid on
axes(handles.axes2);
fw=500;
fv=isosurface(x,y,z,Vol,fw);
p=patch(fv);
set(p,'facecolor','b','edgecolor','none');
patch(isocaps(x,y,z,Vol, fw), 'FaceColor', 'interp', 'EdgeColor', 'none');
colormap('jet')
box on
daspect([1,1,1])
view(3)
set(gca,'zdir','reverse','color',[0.2,0.2,0.2]);
camlight
camproj perspective
lighting phong
axis equal
grid on
```

Generate a grid using meshgrid. Use axes1 to display a slice of the model at the midpoint of its width, and use axes2 to show the model's orientation in three - dimensional space. Then, set relevant parameters such as lighting, viewing angle, and projection method. During the display process, you can use the interactive buttons on the toolbar to observe the geological model represented by the three - dimensional data volume more clearly.

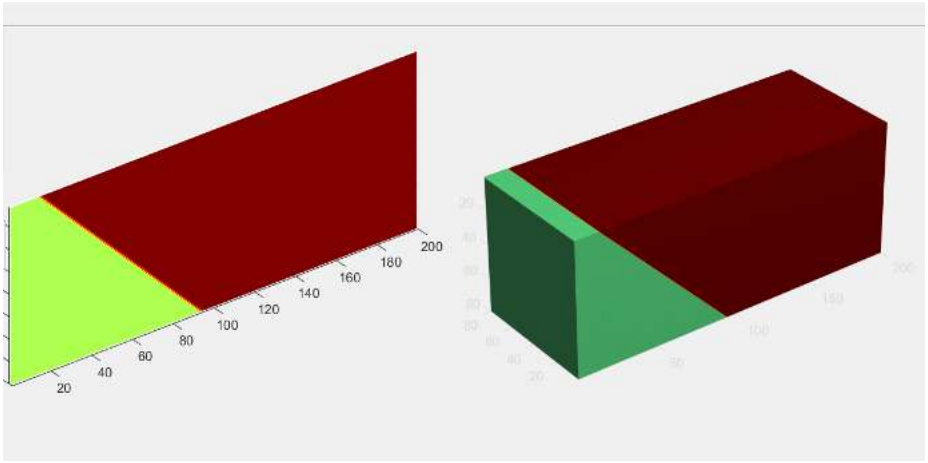

FIG 4. model display

Open the c.exe file in the application directory. The graphical user interface is shown in the following figure. As you can see, there are four types of models to choose from, and you can also read and save three - dimensional data volumes. Here, click the "Karst Cave Model" button. Then, enter the

corresponding parameters as required respectively. This step is a crucial one for creating a three - dimensional scalar data volume, which involves assigning values to the data volume.

After all the data has been set, click "Generate and Display Model". Once you click the button, you will notice that the edge of the button turns blue, which indicates that the program has been executed. Regarding the parameter settings of the tunnel, the central axis of the tunnel is on the central axis of the entire model, and its overall shape is a cuboid with the same width and height. For the parameters of the karst cave, there are the coordinates of the central point and the radius. Its overall shape is a cube with a side length that is twice the radius. The result is shown in the following figure.

The first picture shows a slice of the three-dimensional model at the halfway point of the width of the entire model, and the second picture shows the display of the entire model in space.

At the same time, you will find that three new files have been generated in the folder where the application is located. They are "model_rongdong.vp", "model_rongdong.vs", and "model_rongdong.rho" respectively. These three files are the required three-dimensional scalar data volumes. They record the longitudinal wave velocity, transverse wave velocity, and density data of the geological model respectively.

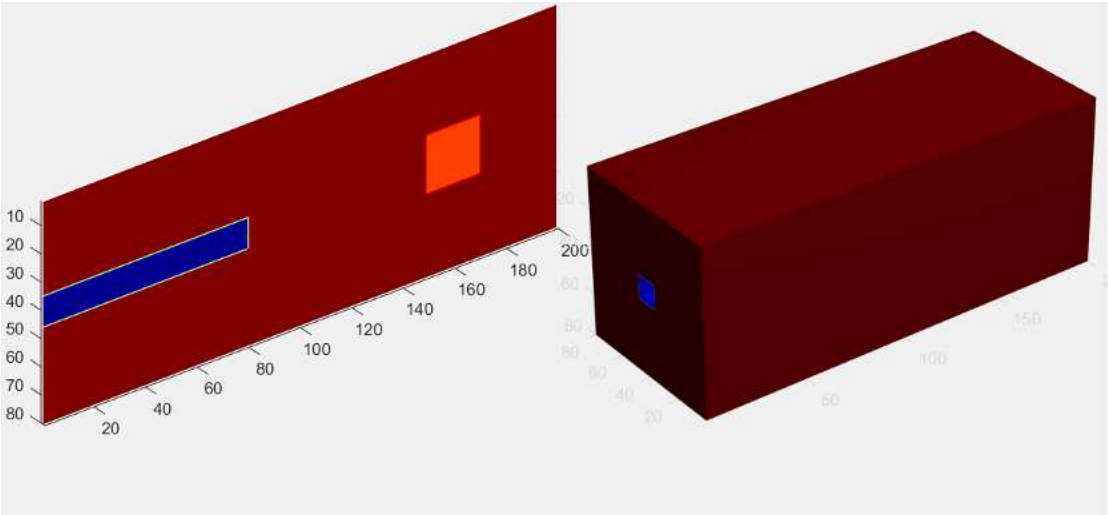

FIG 5. shows the generated model

3. SIMULATION OF SEISMIC WAVE PROPAGATION

Faults are the most common models in advanced detection, and it is meaningful to study their response characteristics. As a layered medium, faults are a widespread structural form. When the stress caused by the extrusion and distortion between rock layers exceeds a certain strength, the rock layers fracture, and there is a relatively obvious displacement between the two contacting rock masses. Faults can be classified into different scales according to their size. Due to the mutual extrusion between rock masses, there is a relatively obvious fractured zone on the contact surface, which is roughly parallel to the fault plane. In such a zone, there are often underground rivers, silt belts, and weak interlayers. In the advanced geological prediction of tunnels, faults are the most common models. During construction, they are often classified into different types according to the relationship between the fault strike and the tunnel axis, including vertical, inclined, and parallel faults. As the main cause of construction disasters during tunnel construction, it is necessary to study faults. Therefore, in this section, fault models with different strikes and densities will be established for numerical simulation.

First, a fault model is established. The size of the model is 500m×80m×80m. The P-wave velocities of the three rock layers are 5700m/s, 4000m/s, and 5000m/s respectively. The S-wave velocities are 3400m/s, 2400m/s, and 3000m/s respectively. The densities are 2200 kg/m³, 1800 kg/m³, and 2000

kg/m³ respectively. The length of the tunnel is 150m, and the center of the tunnel is located at the point (75, 40, 40).

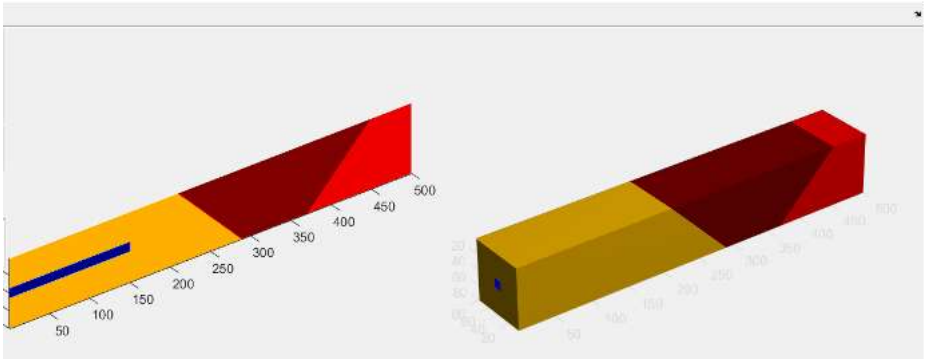

FIG 6. 3d display of the model

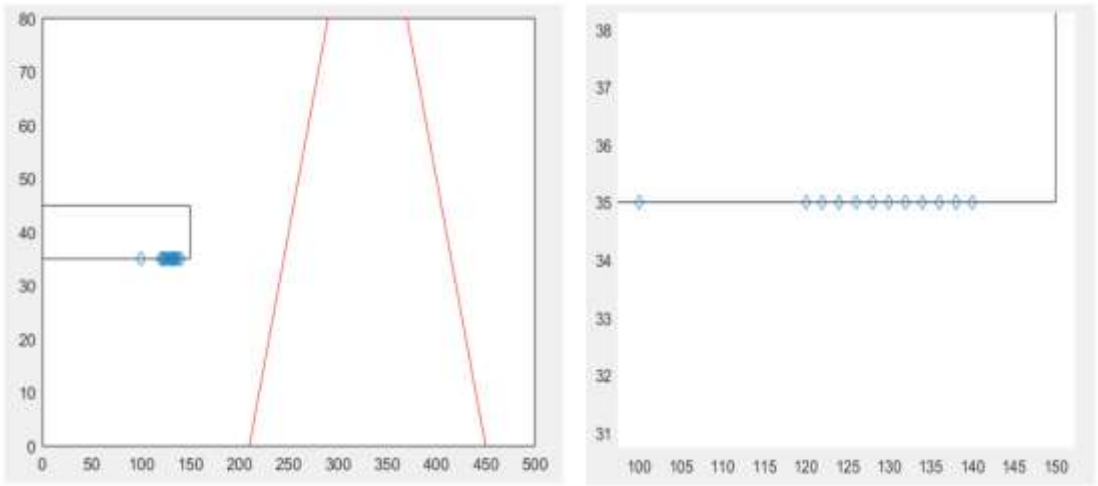

FIG 7. local enlarged view of the observation system and shotpoint detector

For the layout of the observation system of this model: The coordinate of the geophone is (100, 35, 40), and the coordinates of the shot points are (120, 35, 40), (122, 35, 40), (124, 35, 40), (126, 35, 40), (128, 35, 40), (130, 35, 40), (132, 35, 40), (134, 35, 40), (136, 35, 40), (138, 35, 40), and (140, 35, 40) respectively. The design of the observation system is shown in the figure below.

Conduct the simulation of the observation system in the way shown in the figure. After setting the corresponding parameters on the computer, start the forward modeling of the wave field.

It can be seen that the boundary conditions can absorb the wave field very well, and there is no generation of boundary reflections. It can be observed that when the explosive source is excited near the free interface of the tunnel, longitudinal waves (P-waves), shear waves (S-waves), and surface waves formed by interference on the tunnel wall are generated. These waves propagate along the top and bottom surfaces of the tunnel to the other side of the tunnel. Among them, the energy of the longitudinal waves is weak, while the energy of the shear waves and surface waves is strong. As the wave field is extrapolated and the propagation distance increases, the wave field energy attenuates due to spherical divergence.Due to the presence of the tunnel, the wave field has changed significantly compared with that in a homogeneous medium and has become more complex. Relatively speaking, the energy of the direct shear wave is strong, while the energy of the longitudinal wave is weak, and the longitudinal wave quickly propagates out of the computational domain. The surface waves generated by the excitation on one side of the tunnel propagate along the free interfaces of the top and bottom of the tunnel to the other side and will also propagate along the tunnel wall. Then, the direct shear wave propagates to the absorption boundary region. The shear wave energy observed subsequently is mainly caused by the return of the shear wave diffracted by the corner points of the

tunnel by the surface waves. The surface waves and shear waves still account for the main energy. Relatively speaking, the polarity of the shear wave is reversed on the left and right sides of the vertical plane passing through the source, which is consistent with the actual situation.Then, the surface waves propagate to the corner points of the tunnel face, generating diffracted shear waves and surface waves propagating along the free interface of the tunnel. Then, the energy of the diffracted longitudinal waves is weak and not easy to observe. As time is extrapolated, the diffracted shear waves and direct shear waves are superimposed and propagate outward.

The lithological interface is an unfavorable geological structure frequently encountered during tunnel construction. There are often differences in the wave velocities and densities of the surrounding rocks on both sides of the interface, thus forming a wave impedance interface. In addition, the development of fault fracture zones is often accompanied near the interface, which may pose hazards to tunnel construction. Therefore, fully understanding the seismic wave field characteristics of the lithological interface in front of the tunnel and effectively identifying the reflection information of the lithological interface are conducive to the implementation of the advanced seismic prediction for tunnels.

FIG 8. seam needle field test and outcrop

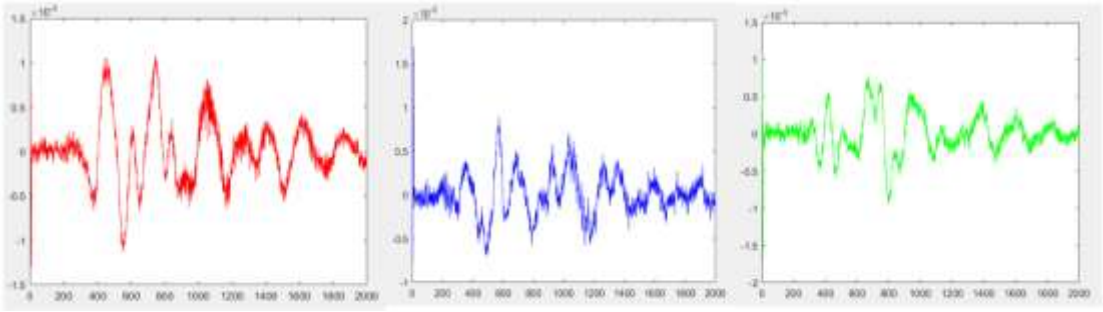

FIG 9. x, y and z component information of the field 10th gun

It can be seen from the figure the on-site measurement process using the TSP2000. This set of rock formations is carbonate rock, with a small portion of it exposed above the ground. During the on-site measurement, the geophone is positioned at the far right of the rock formations. To the left of the entire set of rock formations is soil, and there is an interface right here.

In response to this, I specifically went to the Fengshan Needle Geological Park to find an exposed rock formation that contains a rock formation interface. According to the actual characteristics of the rock formation and the method of experimental data collection, a model was specially designed. The size of the model is 200m×80m×80m. The P-wave velocities of the two rock formations are 3700m/s and 2400m/s respectively. The S-wave velocities are 2400m/s and 1500m/s respectively. The densities are 2200 kg/m^3 and 1800 kg/m^3 respectively. Since it is simulating the actual situation, there is no tunnel. The design of the shot points and geophone points is on the ground. Therefore, the position of the geophone in the model is (100, 0, 2), and the coordinates of the shot points are (75, 0,

2), (73, 0, 2), (71, 0, 2), (69, 0, 2), (67, 0, 2), (65, 0, 2), (63, 0, 2), (61, 0, 2), (59, 0, 2), (57, 0, 2) respectively.

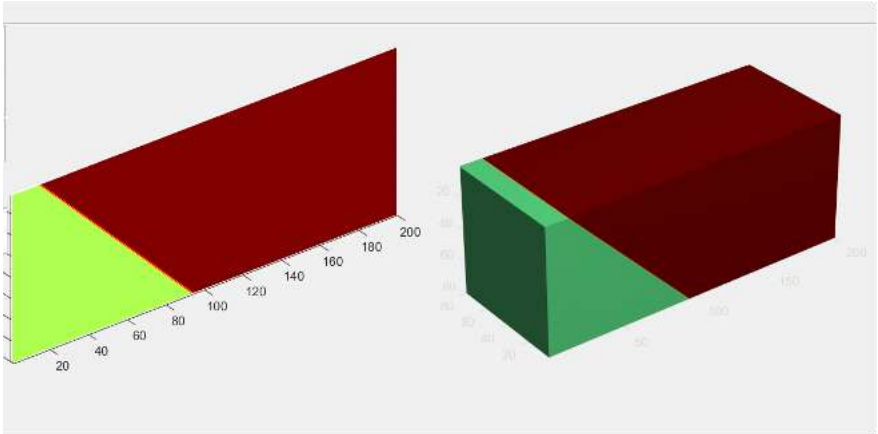

FIG 10. model of an exposed rock stratum

After setting the parameters on the computer according to the above description, the forward modeling simulation is carried out. The finite element PML boundary conditions based on the second-order displacement equation used in the wave field forward modeling simulation can effectively attenuate and absorb the three-dimensional tunnel wave field in the boundary area, and there is no generation of boundary reflections, which provides a basis for accurately obtaining the characteristics of the wave field response.The direct wave generated by the source excited on the side wall of the rock formation propagates through the top and bottom interfaces to the side wall on the other side. Then the direct longitudinal wave arrives first. With the extrapolation of the wave field, it can be seen that the reflected longitudinal wave and the transmitted longitudinal wave with relatively strong energy are generated when the direct longitudinal wave passes through the interface. A converted shear wave with weaker energy can be observed behind.During the propagation of the wave field, the direct wave or the transmitted wave accounts for the main energy, and the energy of the interface reflected wave is weak. Therefore, it is crucial to effectively identify the reflected wave of the interface in the seismic record.

Through the simulation of the lithological interface with an inclination angle, it can be known that the energy of the reflected shear wave generated by the lithological interface is relatively stronger than that of the reflected longitudinal wave. Among the three components, the energy of the uy component is the weakest. In the uz component, the energy of the reflected longitudinal wave is stronger than that of the ux and uy components, while in the ux component, the energy of the reflected shear wave is stronger than that of other components.

Therefore, in the advanced seismic prediction of tunnels, comprehensively utilizing multi-component seismic data to carry out multi-wave exploration, especially shear wave exploration, will help improve the reliability and accuracy of the prediction. In addition, with the change of the inclination angle, the shape of the reflected wave tilts towards the up-dip direction of the interface. Effectively identifying the shape of the reflected wave in the actual record will help determine the dip direction of the interface in front of the tunnel.

It can be found that the comparison diagrams of the waveforms are not exactly the same. In actual situations, since it is an artificially excited source, each excitation may be slightly different. An obvious difference can be observed in reality. The dip angle of the stratum in the model is inconsistent with the actual situation, and the propagation speed is also inconsistent with the actual one. Overall, the energy of the seismic waves decreases from strong to weak.

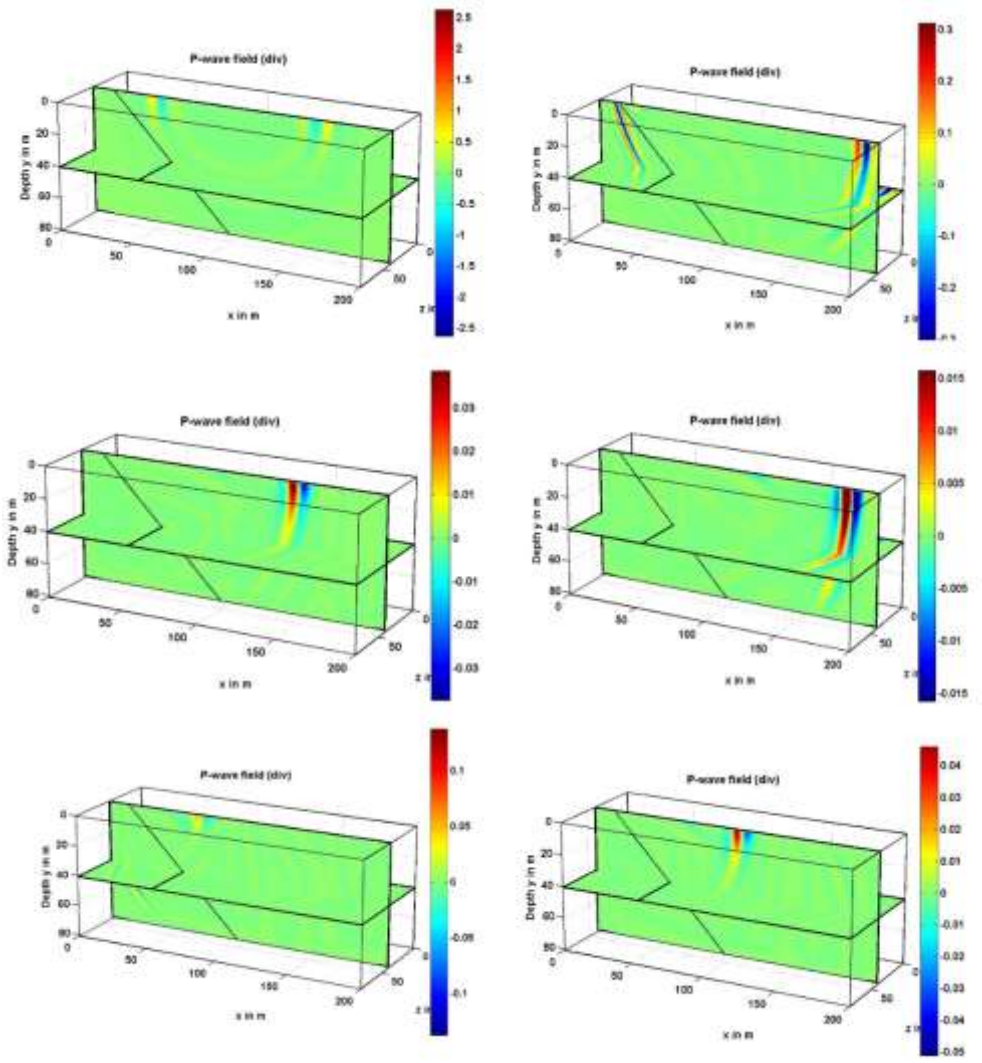

FIG 11. wave field snapshots of seismic waves at different moments during model propagation

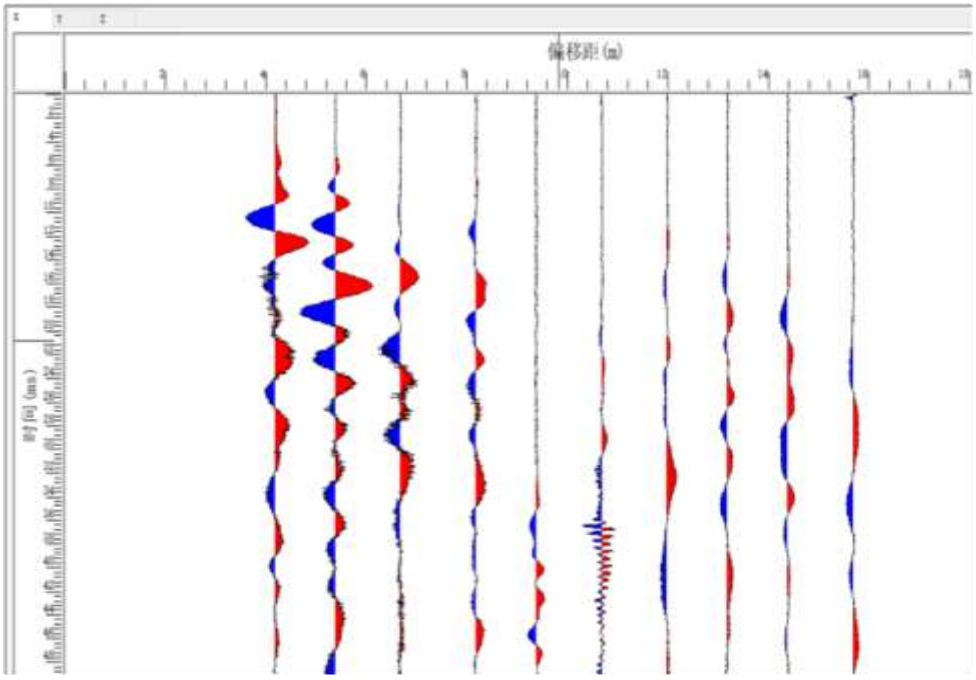

FIG 12. actual seismic wave plane figure

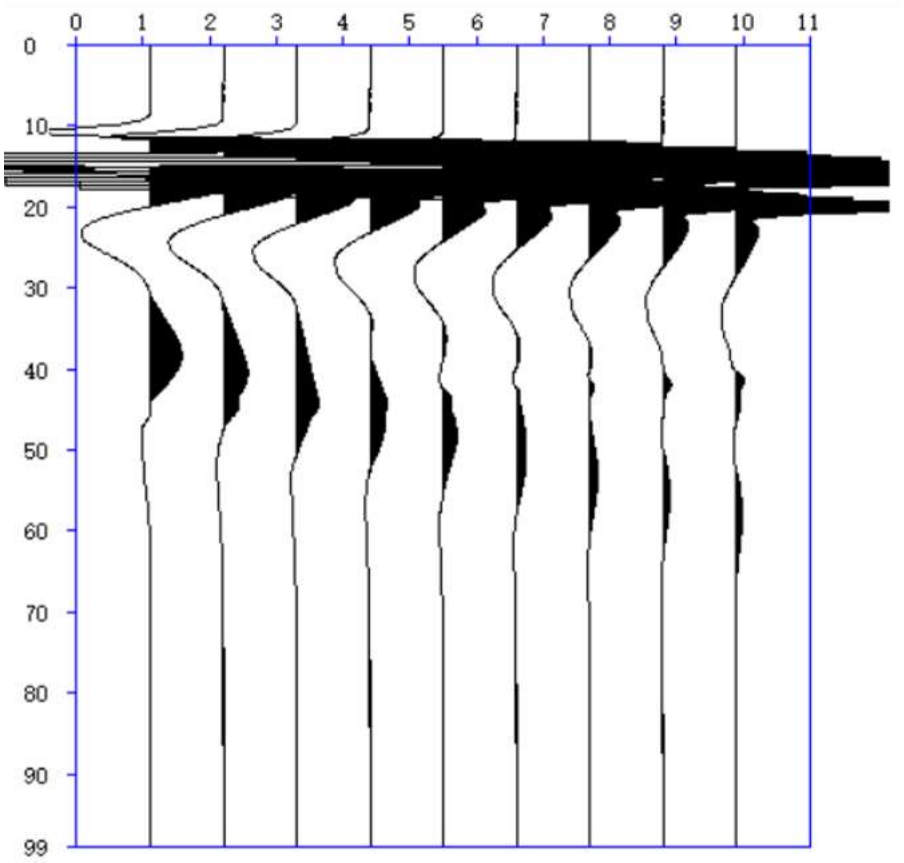

FIG 13. seismic wave plane diagram of forward model

4. CONCLUSIONS

This paper, combined with the geological abnormal bodies that may actually be encountered in tunnel advanced detection and based on the previous research on tunnel advanced detection, conducts three-dimensional modeling and numerical model research on the unfavorable geological bodies that may be encountered in the driving roadway. Through comparative analysis and summary, it is hoped to have certain guiding significance for the theory and engineering application of tunnel advanced detection.Although domestic and foreign scholars have carried out certain research work on the advanced detection of geological anomalies such as faults, there are still many deficiencies in the research so far. It is necessary to continuously combine theoretical research with on-site detection work and continuously deepen and improve the understanding.

Based on the three-dimensional finite element forward modeling and absorption boundary conditions, and according to the structural characteristics of the lithological interface of unfavorable geological bodies commonly encountered during tunnel construction, a three-dimensional tunnel geological and geophysical model is constructed using self-developed modeling software, and the three-dimensional elastic wave full-wavefield simulation of the tunnel wave field is realized. It mainly analyzes the propagation law of the three-dimensional seismic wave field of the tunnel in the lithological interface model in front of the tunnel, and enhances the systematic understanding of the propagation characteristics of the tunnel wave field.

REFERENCES

[1] Wu W ,Wei Z ,Tao L .Compression of seismic forward modeling wavefield using TuckerMPI[J].Computers and Geosciences,2023,172

[2] Jianjun X ,Dandan C .FCT finite difference forward simulation of the submarine viscoelastic seismic wavefield[J].IOP Conference Series: Earth and Environmental Science,2021,660(1):012111-.

[3] M D V ,C B ,L K , et al.Accelerating numerical wave propagation using wavefield adapted meshes. Part I: forward and adjoint modelling[J].Geophysical Journal International,2020,221(3):1580-1590.

[4] BlackshireL J .Forward ultrasonic model validation using wavefield imaging methods[J].AIP Conference Proceedings,2018,1949(1):020012.

[5] Jia X ,Yang L .A memory-efficient staining algorithm in 3D seismic modelling and imaging[J].Journal of Applied Geophysics,2017,14362-73.

[6] Computational Physics; Reports from University of Houston Highlight Recent Findings in Computational Physics (Forward Scattering and Volterra Renormalization for Acoustic Wavefield Propagation in Vertically Varying Media)[J].Journal of Technology & Science,2016,

[7] Yao J ,Lesage A ,Hussain F , et al.Forward Scattering and Volterra Renormalization for Acoustic Wavefield Propagation in Vertically Varying Media[J].Communications in Computational Physics,2016,20(2):353-373.

[8] Fu L ,Mu Y ,Yang H .Forward problem of nonlinear Fredholm integral equation in reference medium via velocity-weighted wavefield function[J].Geophysics,2012,62(2):650-656.

[9] Tromp J ,Luo Y ,Hanasoge S , et al.Noise cross-correlation sensitivity kernels[J].Geophysical Journal International,2010,183(2):791-819.

[10] Nita G B .Forward Scattering Series and Padé Approximants for Acoustic Wavefield Propagation in a Vertically Varying Medium[J].Commun. Comput. Phys.,2008,3(1):180-202.

[11] Kees W J Z .Wavefield extrapolation and prestack depth migration in anelastic inhomogeneous media[J].Geophysical Prospecting,2002,50(6):629-643.

[12] Chapter 14 Integral representations in wavefield theory[J].Methods in Geochemistry and Geophysics,2002,36443-465.

[13] LICHMAN E .INFORMATIONAL CAPACITY OF ACOUSTIC MEASUREMENTS[J]. Journal of Computational Acoustics, 2001,9(4):1395-1406.